Materials Science & Engineering C 120 (2021) 111784

Contents lists available at ScienceDirect

Materials Science & Engineering C

journal homepage: www.elsevier.com/locate/msec

Ohmic heating as a new tool for protein scaffold engineering

Rui M. Rodrigues *, Ricardo N. Pereira, António A. Vicente, Artur Cavaco-Paulo, Artur Ribeiro

CEB-Centre of Biological Engineering, University of Minho, 4710-057 Braga, Portugal

ARTICLE INFO

Keywords:
Gelation
Scaffolds
Electric filed
Tissue engineering
Cell proliferation

ABSTRACT

Ohmic heating (OH) is recognised as an emerging processing technology which recently is gaining increasing attention due to its ability to induce and control protein functionality. In this study, OH was used for the first time in the production of scaffolds for tissue engineering. BSA/casein solutions were processed by OH, promoting protein denaturation and aggregation, followed by cold-gelation through the addition of Ca^{2+}. The formation of stable scaffolds was mostly dependent on the temperature and treatment time during OH processing. The variations of the electric field (EF) induced changes in the functional properties of both gel forming solutions and final scaffolds (contact angle, swelling, porosity, compressive modulus and degradation rate). The scaffolds' biological performance was evaluated regarding their ability to support the adhesion and proliferation of human fibroblast cells. The production process resulted in a non-cytotoxic material and the changes imposed by the presence of the EF during the scaffolds' production improved cellular proliferation and metabolic activity. Protein functionalization assisted by OH presents a promising new alternative for the production of improved and tuneable protein-based scaffolds for tissue engineering.

1. Introduction

Ohmic heating (OH) is an emerging technology with great potential and applicability in the food and biotechnological industry [1–4]. This technology relies on the passage of electric current on a semi-conductive matrix (e.g. foodstuff or biomaterial), resulting in direct heat deposition and, thus, in a fast and homogeneous heating with high energetic efficiency [5]. Furthermore, the use of OH demonstrated the capacity to induce specific changes in biomolecules resultant from the action of the altering electric field. In fact, the action of moderate electric fields (MEF) associated with OH technology has been gaining interest in protein functionalization, namely by their ability to disturb the protein-unfolding pathways, promote specific structural changes, and influence the protein's aggregation and gelation profiles. The use of OH can changes protein structure and its interactions, affects the size and shape of protein's aggregates, and thus gives rise to protein-based systems with a distinctive morphologies, viscoelastic behaviour, water retention and swelling behaviour [6–9]. All of this suggests that OH can be exploited in inducing and controlling supramolecular structure formation by globular proteins, assisting in the development of distinctive protein-based systems.

There is a growing interest on the use of proteins as building-blocks for the development of biomedical applications, such as controlled delivery systems and scaffolds for tissue engineering [10–13]. Particularly regarding scaffold production, several fabrication techniques – e.g. freeze-drying, solvent casting, foaming, electrospinning or 3D printing – have been used to attain desired functional properties [14,15]. Associated with these fabrication techniques, protein functionalization is a necessary step, being usually achieved by chemical modification, enzymatic hydrolysis or crosslinking through the use of strong reducing agents. The use of these strategies may bring negative implications since some of these agents and modifications present toxicity or low biocompatibility issues [14,16,17]. Physical modification of proteins and other methodologies to control protein aggregation and gelation offer interesting possibilities on the formation of protein-based systems with improved performances. Despite the literature available on the subject in other areas (e.g. food-related applications), the process is yet to be fully exploited in biomaterials and biomedical applications. A particular methodology often used to create protein gels is the cold-induced gelation, where proteins in solution are denatured and aggregate, followed by a gelation induction step at room temperature. Gel formation is achieved by changing the electrostatic balance of these aggregates suspensions by modifying the solution's pH or by adding salts, resulting in enhanced protein/aggregates interactions and, therefore, in the formation of a network yielding a gel [18,19]. The possibility of independently controlling the processes of aggregation and gelation,

* Corresponding author.
E-mail address: ruirodrigues@ceb.uminho.pt (R.M. Rodrigues).

https://doi.org/10.1016/j.msec.2020.111784
Received 15 September 2020; Received in revised form 11 November 2020; Accepted 2 December 2020
Available online 10 December 2020

allows the gel to be casted onto an intended shape and results on highly tuneable gels with distinctive characteristics [20,21]. Ribeiro et al. [22,23] have successfully adopted this process to develop scaffolds for tissue engineering, using a combination of globular proteins - i.e. bovine serum albumin (BSA) or human serum albumin (HSA) - and alpha-casein, a smaller and amorphous protein. The developed process relied on a mild thermal processing and the use of ditiotreitol (DTT) as a reducing agent in order to further destabilize the protein structure, followed by Ca^{2+} addition to induce crosslinking. In fact, DTT is commonly used in gel preparation processes and has been applied to the development of scaffolds and other biomedical applications [24,25]. However, DTT by itself or in synergy with other media constituents may compromise cell viability and needs to be eluted from the scaffolds [26–28]. Alternatively, the initial denaturation step could be optimized to potentiate protein-protein interactions and improve the gelation process, possibly eliminating the use chemical agents such as DTT.

In view of this possibility, the present study intended to explore the potential of OH to assist the production of protein-based scaffolds for tissue engineering, previously established by Ribeiro et al. [22]. It was our goal to optimize the thermal treatment conditions in order to promote the formation of stable scaffolds without the use of reducing agents. Along with this optimization, the use of OH, its potential to tune protein functional properties and its impact in the performance of the scaffolds was evaluated for the first time.

2. Materials and methods

2.1. Materials

All reagents were of analytical grade and purchased from Merck-Sigma (Spain). BSA and casein sodium salt from bovine milk were used without further purification and milli-Q water was used for the preparation of all solutions.

2.2. Preparation of the scaffolds

The scaffolds were obtained by salt-induced cold gelation in the presence of calcium chloride ($CaCl_2$) at pH 7.07. Shortly, protein solutions of BSA in water and casein in Tris 5×10^{-2} mol.L^{-1}, pH 7.4, were prepared separately and mixed to the final concentration of 4.19% (w/v) of BSA and 0.69% (w/v) of casein. The solutions were thermally treated to promote protein denaturation and aggregation; cooled down to room temperature for 1 h and finally $CaCl_2$ (to a final concentration of 0.1 mol.L^{-1}) was added. The mixtures were stirred to homogenize the samples, and were casted on 48-well plates and left gel for 12 h. The samples were frozen at −20 °C and freeze dried to remove the solvent completely. The resulting scaffolds with a diameter of 10 mm and a height of 5 mm were kept on a desiccator at room temperature until further use.

2.3. Thermo-electric treatments and experimental design

Thermal treatments were performed in a double-jacketed glass cylinder containing stainless steel electrodes at each edge, as described by Rodrigues et al. [29]. For conventional heat exchange treatments (where no EF was applied) temperature was controlled by circulating water in the vessel jacket from a thermo-stabilized water bath. For the OH treatments, the temperature was controlled by regulating the voltage output of a function generator at an electrical frequency of 25 kHz (1 Hz–25 MHz and 1–10 V; Agilent 33220A, Penang. Malaysia) which was then amplified in an amplifier system (Peavey CS3000, Meridian, MS, USA). Temperature was measured with a type K thermocouple (Omega Engineering, Inc., Stamford, CT, USA), connected to a data logger (USB-9161, National Instruments Corporation, Austin, TX, USA). The samples were magnetically stirred during the treatments to ensure homogeneity.

In order to optimize the scaffolds' production conditions, some preliminary tests were undertaken using a Box-Behnken design with 3 factors in 3 levels. The factors selected were temperature, treatment time and EF applied, on intervals of 70 to 85 °C, 5 to 30 min and 0 to 40 V.cm^{-1}, respectively. These conditions were selected based on the following criteria: 70 °C is the denaturation temperature of BSA and 85 °C was found to be the limit temperature before the occurrence of the thermal gelation of the protein solutions; the maximum treatment time was 30 min as this was the time necessary to reach equilibrium in the aggregation process; the maximum EF of 40 V.cm^{-1} was established by the maximum voltage output yielded by the system, given the electric conductivity of the solution and the defined temperature range. The response variables for the optimization were the in vitro degradation, swelling and porosity of the obtained scaffolds. These criteria were selected since it was aimed at obtaining stable structures with maximum porosity (to loge cells) and high swelling ratio to uptake culture medium, thus allowing cellular growth. The desirability function analysis (DFA) derived from the model was applied to estimate a desirability value, i.e. a measure of how close the fitted value is to a desired value within pre-established limits [30].

2.4. Characterization of the gel-forming solutions

In order to improve the understanding of the EF effects on the protein denaturation and aggregation process, a characterization of the gel-forming solutions was performed after the OH treatments.

2.4.1. Fluorescence determination

Fluorescence determinations were performed on the fluorescence instrument Aqualog (HORIBAJobin Yvon, Inc. Japan). Intrinsic fluorescence of the protein solutions was determined by exciting the Trp in the samples at 295 nm and recording the emission from 300 to 450 nm. 8-anilino-1-naphthalenesulfonic acid (ANS) was used as a conformational probe. ANS stock solution (1.2×10^{-2} mol.L^{-1}) was prepared in methanol and added to the protein test solution at a final concentration of 5×10^{-4} mol.L^{-1}. The mixture was excited at 370 nm the fluorescence emission at 480 nm was recorded.

2.4.2. Determination of free thiol groups

Free thiol groups (SH) determination was performed using Ellman's DTNB (5.5′-dithiobis-(2- nitrobenzoicacid)) method [31]. On a glass test tube 2.5 mL of phosphate buffer (0.1 mol.L^{-1}, pH 8), 0.5 mL of protein solution and 100 μL of DTNB solution (5×10^{-3} mol.L^{-1}) were mixed and allowed to react for 1 h at room temperature. The absorbance at 412 nm was determined on a UV-VIS spectrophotometer (V-560, Jasco Inc., Tokyo, Japan). All determinations were performed in triplicate and the absorbance of the blank (using buffer instead of protein solution) was subtracted to each sample's absorbance.

2.4.3. Particle size determinations

The hydrodynamic radius of the protein aggregates were determined by dynamic light scattering (DLS) using a Zetasizer Nano (ZEN 3600, Malvern Instruments Ltd., Malvern, U.K.) Samples of proteins aggregates were diluted at 1:10 and 1 mL of the resulting dilute solution were poured into disposable sizing cuvettes, the temperature of the cell was maintained at 25 ± 0.5 °C during the measurement. The poly-dispersity index (PDI) derived from cumulant analysis of the DLS measurements was also evaluated, describing the width or the relative variance of the particle size distribution. All measurements were carried out at least in triplicate.

2.5. Scaffolds characterization

2.5.1. Functional properties and stability

2.5.1.1. In vitro degradation. The obtained scaffolds were incubated in Phosphate-Buffered Saline (PBS) solution at 37 °C for a period of 15

days. Solutions were changed every 24 h and at designated time points, samples were recovered, washed with distilled water, dried in a desiccator, and weighed. The extent of degradation was estimated according to Eq. (1).

$$Weight\ loss\ (\%) = \left(\frac{(m_i - m_f)}{m_i}\right) \times 100 \quad (1)$$

where m_i is the initial dry mass and m_f is the final dry mass of the sample.

2.5.1.2. Swelling ratio. Dry scaffolds were submerged in PBS buffer at 37 °C and left for 24 h. The samples were recovered, the excess of buffer was gently removed with a filter paper and the wet weight of the scaffolds was determined. The swelling ratio was calculated according to Eq. (2).

$$Swelling\ ratio = \frac{Ws - Wd}{Wd} \quad (2)$$

where *Ws* is the mass of the swollen material, and *Wd* is the initial dry mass.

2.5.1.3. Porosity. The porosity of the scaffolds was determined by a similar procedure to the swelling degree but using distilled water. The porosity values were obtained according to Eq. (3).

$$Porosity\ (\%) = \left(\frac{Ws - Wd}{dw}\right) \times \frac{100}{V} \quad (3)$$

where *Ws* and *Wd* are the mass of the swollen and lyophilized scaffold, respectively, *dw* is the density of water, and *V* is the volume of the scaffold in the swollen state.

2.5.1.4. Microstructural morphology. The samples were characterized using a desktop scanning electron microscope (SEM) (Phenom-World BV, Netherlands). All results were acquired using the ProSuite software. The samples were placed on aluminium pin stubs with electrically conductive carbon adhesive tape (PELCO Tabs™) and gently blown with compressed air to remove detached material; no coating was used on the imaging process. The aluminium pin stub was then placed inside a Phenom Charge Reduction Sample Holder. The analysis was conducted at 5 kV with intensity image.

2.5.1.5. Contact angle. Contact angle measurements were performed in a Data Physics OCA20 device. The tests were conducted at room temperature and ultrapure water was used as test liquid. The contact angles were measured by depositing water drops (3 μL) on the sample surface and analysed with SCA20 software. At least five measurements in each sample were performed in different scaffold surface locations and the average contact angle was taken as the result for each sample.

2.5.1.6. Mechanical properties. Mechanical properties were determined by uniaxial compression measurements using a TA HD Plus Texture Analyzer (Stable Micro Systems. UK) with an aluminium 25 mm probe. Prior to mechanical tests, the scaffolds were hydrated in PBS for 24 h at room temperature, the excess of liquid was gently removed with filter paper and placed on the texture analyzer platform. At least 10 samples of each experimental condition were tested using a trigger force of 0.05 N and a crosshead speed of 1 $mm.s^{-1}$.

The compressive modulus was calculated from slope of the linear fit of the stress–strain curve between 10 and 20% strain.

2.6. Cell culture

Normal human skin fibroblasts immortalized by overexpression of telomerase (BJ-5ta cell line) were maintained according to ATCC recommendations (four parts of Dulbecco's modified Eagle's medium (DMEM) containing 4 mmol/L-glutamine, 4.5 $g.L^{-1}$ sodium bicarbonate and 1 part of Medium 199, supplemented with 10% (v/v) of foetal bovine serum (FBS), 1% (v/v) of penicillin/streptomycin solution and 10 $g.mL^{-1}$ hygromycin B). Cells culture was incubated at 37 °C in a humidified atmosphere with 5% CO_2, and the culture medium was replaced every 2 days.

2.6.1. Cytotoxicity evaluation

BJ-5ta cells were used as model of general cytotoxicity. Degradation and leachable products from the scaffolds were used to evaluate cytotoxicity. The scaffolds were disinfected by immersion three times in PBS containing 1% (v/v) penicillin/streptomycin for 20 min, followed by immersion in sterile PBS for 30 min to remove any remaining penicillin/streptomycin present on the scaffold microstructure. The disinfected scaffolds were incubated in 2 mL of medium at 37 °C for 24 h, the medium was recovered and used as conditioned media. Cells seeded (10×10^3 cells/100 μL/well) on 96-well tissue culture polystyrene plates the day before experiments, were exposed to the conditioned medium and were further incubated at 37 °C in a humidified atmosphere with 5% CO_2. Cells exposed to culture medium incubated without the presence of the scaffolds were used as control of the effect of the scaffolds' leachables. Metabolic viability was assessed at the end of 24 and 48 h of contact, using the MTT (3-(4,5-dimethylthiazol-2-yl)-2,5-diphenyltetrazoliumbromide) assay [32].

2.6.2. Cell culture in the scaffolds

The scaffolds were disinfected and equilibrated for 24 h at 37 °C in medium without FBS prior to cell seeding. The scaffolds were carefully placed in 24-well plates and 200 μL of cell suspension (5×10^5 cells. mL^{-1}) were poured onto the top of each scaffold and allowed to infiltrate. After 2 h incubation, fresh complete medium (1 mL) was added to each scaffold and the samples were incubated for either 120 or 192 h, with half of the culture medium being renewed every 2 days.

The quantification of the number of cells on the cell-scaffold constructs were determined by DNA quantification with the Hoechst 33258 assay (Invitrogen, CA) according with previous reports [22,23]. After each indicated time point, cells/scaffold constructs were collected, rinsed with PBS and the cells were harvested by incubating with a 0.25% solution of trypsin. Cells were then collected by centrifugation and lysed in a Tris 15 $mmol.L^{-1}$ pH 7.4 buffer with successive frozen-thawing cycles. Cell lysates were incubated with 5 $mg.mL^{-1}$ Hoechst 33258 solution at 1:1 ratio, for 40 min at room temperature in 96-well black plates. Fluorescence was determined at 350 nm excitation and 445 nm emission. The relative fluorescence unit value obtained from samples was interpolated against a DNA standard curve constructed using known number of cells, to determine the DNA content/number of cells in each sample.

The influence of scaffold's properties on cell metabolic activity was evaluated using the MTS method. The MTS cell proliferation assay is a colorimetric sensitive quantification of viable cells in proliferation and cytotoxicity assays [33]. At the end of the defined time points, the cells/scaffold constructs were collected to a new 24-well plate and 1 mL of fresh medium with MTS was added to each well. The cells/scaffolds were incubated for 4 h at 37 °C in a humidified atmosphere with 5% CO_2, and the absorbance was measured at 490 nm. Scaffolds without cells were used as control for the influence of the constructs' components on the MTS protocol. The relative absorbance unit value obtained from samples was interpolated against a MTS standard curve made using known number of cells.

Cell adhesion was further assessed by SEM for a detailed visualization of cell-material interactions. For SEM analysis, the cells/scaffolds constructs were soaked in a fixation solution (1 mL of 2.5% glutaraldehyde (Merck) in PBS) for 1 h at room temperature, rinsed with distilled water and dehydrated by immersion for 30 min in a series of successive ethanol-water solutions (55%, 70%, 80%, 90%, 95% and 100% v/v of ethanol). The samples were then dried at room temperature

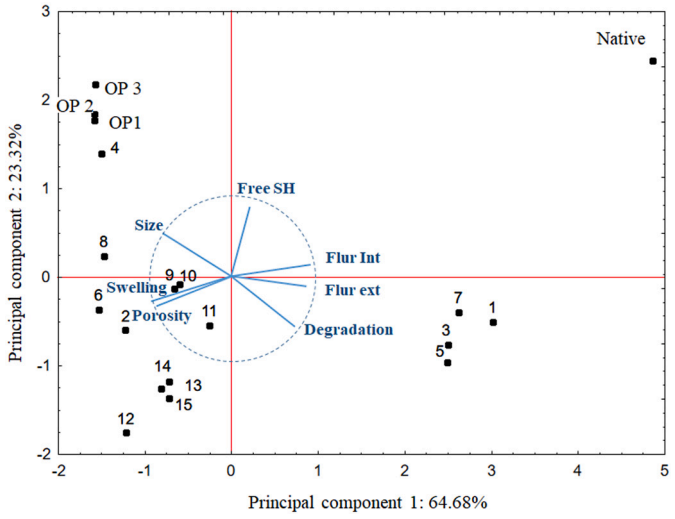

Fig. 1. Principal component analysis of the experimental design points (1–15), the produced scaffolds at the optimal conditions under 1 V.cm^{-1} (OP1), 20 V.cm^{-1} (OP2) and 40 V.cm^{-1} (OP3), and unheated (native) protein solution.

and coated with a thin gold layer using a sputter coater prior to SEM analysis.

2.7. Data analyses

All data analysis, fitting, plotting and statistical test procedures were performed on the Statistica package software version 10.0.228.8 (StatSoft Inc.). For the preliminary tests used to determine the best condition for the scaffold's formation, a Box-Behnken experimental design was performed and a desirability function analysis (DFA) derived from the RSM model was applied to estimate a desirability value, i.e. a measure of how close the fitted value is to a desired value within pre-established limits [30,34].

A principal component analysis (PCA) was performed to identify a global pattern of the samples distribution and correlate the large amount of data from de structural characterization of the proteins' suspensions and the functional properties of the scaffolds.

Once found the optimal conditions for the scaffolds formation, samples produced at different EF values were further analysed by applying an analysis of variance to estimate any statistically significant differences at a confidence level of 95%.

3. Results and discussion

The design of a scaffold depends on the tissue to be engineered, specificities for intended mechanical properties and type of cell to be cultivated. Regardless of the specific application, the biomaterial must present a certain stability and provide support for cellular proliferation and maintenance of cells metabolic activity. This work aimed at optimizing the process of protein functionalization, assisted by OH, in order to produce biomaterials suitable for tissue engineering. Starting from the formulations previously described by Ribeiro et al. [22,23], OH was implemented as processing technology and its operational conditions, namely temperature, treatment time and voltage gradient applied were optimized in order to promote protein denaturation and aggregation, followed by cold-gelation and free-drying to obtain stable structures with high porosity and swelling capacity. This optimization favoured the intramolecular interaction among protein and aggregates, thus producing stable structures without the use of reducing agents. The results from the experimental design and DFA analysis are presented as supplementary material. Shortly, the temperature was the most decisive factor influencing the optimization, only the temperature of 85 °C allowed the formation of stable scaffolds. Experimental design treatments carried at 70 °C did not originate self-supporting gels and thus it was not possible to produce stable scaffolds in these conditions. The intermediate temperature of 77.5 °C produced self-supporting gels and scaffolds, but they presented high degradation rates and were not stable during the testing procedures. Treatment time was negatively correlated with the degradation of the scaffolds, being observed a decrease in the degradation rate with the increase of the treatment time. The variation of the EF did not determine the formation of stable scaffolds at 85 °C, but it affected the scaffolds' functional properties. The intensity of the EF during the denaturation/aggregation process increased the scaffold degradation rate and this was positively correlated with the increase of scaffolds' swelling and porosity. For further testing, the conditions of 85 °C, 30 min of treatment were used and the EF intensity changed at different levels, accessing its potential to tune the scaffold's functional properties driven by EF action. In order to better understand the correlation between the structural changes imposed by the processing and the characteristics of the produced scaffolds, the native protein solution (control), aggregates solution obtained after thermo-electric treatments and scaffolds properties (i.e. swelling, porosity and degradation) were subjected to a principal component analysis (PCA) represented in Fig. 1.

In the PCA, the seven variables under analysis were reduced to two principal components, which account for 88% of the samples' variability. This allowed representing the data points correspondent to each treatment condition on a two-dimensional projection and evaluating their relationship according to their positioning. At the centre of the referential it is represented the variable correlation plot, showing the magnitude and direction of the influence of each individual variable on the composition of the principal components. The untreated protein solution was isolated from all the OH treated samples on the upper corner of the plot. For this solution, degradation was considered to be 100%, swelling and porosity were considered to be zero. Besides, the sample was characterized by high levels of free SH groups, high intrinsic fluorescence, and low surface hydrophobicity, characteristic of non-denatured protein solutions. Treatment conditions that did not originate self-supporting networks (samples treated at 70 °C, i.e. 1, 3, 5, and 7) could not be tested for degradation, swelling and porosity, thus these variables were also considered to be 100%, zero and zero respectively. This group of treatments were distinguished from the unheated protein solution by the reduction of the free SH groups, intrinsic and extrinsic fluorescence and size increase when compared with the unheated solution. The changes are consistent with the occurrence of low levels of protein denaturation and aggregation. The remaining samples correspond to the ones that formed self-supporting networks, and are positioned on the left side of the projection plot. Their positioning was influenced by low degradation, positive swelling and porosity but also by the particle size increase and fluorescence intensity reduction. These changes are consistent with significant structural changes induced by the treatments at higher temperatures. The optimal points (OP1, OP2, OP3) and the point 4 of the experimental design (with equivalent treatment conditions, i.e. treated at 85 °C for 30 min) were positioned at the left and upper part of the distributions, corresponding to the scaffolds produced by larger aggregates and with lower degradation. The remaining scaffolds placed on the negative *yy* and *xx* quadrant of the projection were less stable but presented higher swelling and porosity. This analysis demonstrates that structural modification can be used to modulate the functional properties of a protein system, and thus give rise to the formation of stable scaffolds with the desired properties. The major advance of this process, compared with previous strategies used for scaffolds formation, is the use of just physical methods avoiding the use of DTT as reducing agent or other chemical compounds, and thus decreasing the potential toxicity resulting from its presence.

3.1. Gel forming solutions characterization

Protein solutions, untreated and treated at 85 °C for 30 min under

Table 1
Intrinsic fluorescence, surface hydrophobicity, free thiol groups and aggregates size, of the gel forming solutions, untreated and treated at 1 V.cm^{-1}, 20 V.cm^{-1} and 40 V.cm^{-1}.

	Fluorescence int./a.u.	Surface hydrophobicity/a.u.	Free thiol groups/μM	Size/nm
Untreated solution	9355.22 ± 14.78^{a}	9439.88 ± 88.25^{a}	211.46 ± 22.78^{a}	115.77 ± 1.14^{a}
EF 1 V.cm^{-1}	7126.01 ± 16.96^{b}	1482.29 ± 14.82^{b}	248.81 ± 9.82^{b}	77.50 ± 0.84^{b}
EF 20 V. cm^{-1}	6927.87 ± 51.34^{c}	1607.98 ± 44.87^{bc}	256.83 ± 12.31^{b}	74.42 ± 0.33^{c}
EF 40 V. cm^{-1}	6813.23 ± 16.09^{d}	1642.15 ± 89.78^{c}	287.34 ± 11.63^{c}	70.33 ± 0.59^{d}

For each column, different letters (a-d) indicate a statistically significant different between samples ($p < 0.05$).

different EF intensities were analysed in terms of intrinsic fluorescence, surface hydrophobicity, free thiol groups content and aggregates size. This analysis allowed to determine the treatment's effect on the denaturation and aggregation profiles of the protein solutions and the impact of the different EF intensities used, prior the cold gelation process.

The intrinsic fluorescence and surface hydrophobicity, determined by the fluorescence of the ANS hydrophobic probe, revealed a substantial decrease after the processing step (Table 1). Particularly for the surface hydrophobicity, it is possible to imply that the hydrophobic groups of the proteins might have been occluded by the establishment of hydrophobic interactions, characteristic of the protein aggregation processes. For the treated samples, differences were observed among the different EF intensities applied, suggesting changes on proteins conformation. These changes are the result of different positioning of the amino acid residues within the proteins/aggregates as well as in different exposure of hydrophobic pockets. This highlights the capacity of the EF to influence the denaturation and aggregation processes, which may have an impact on the network formation and on the scaffolds' functional properties. OH treatments also induced an increase of the free thiol groups content, which is positively correlated with the increasing intensity of the EF used. This increase may be related with a structural rearrangement of the protein molecules when exposed to thermal stress potentiated by the EF action. These changes in free thiol content can also be the result of different aggregation mechanisms, where other interactions (e.g. hydrophobic, electrostatic, hydrogen bonds) are favoured against disulphide bonds. In practical terms, the change on the free thiol content implies changes not only on the aggregates properties, but also on the network formation and final gel properties. The aggregates size was also reduced by the treatments and comparing with the unheated solution the polydispersivity index decreased as the distribution shifted from a polymodal to a monomodal peak (results not shown). The increase on the EF used during the treatment also resulted on the reduction of the aggregates size. These results demonstrate the effect of the treatment on the gel forming solutions and highlight the ability of the EF's applied during OH processing to change protein functionality.

3.2. Scaffolds characterization

3.2.1. Morphology and microstructure

The obtained scaffolds, regardless of the condition used in their production, presented a white colour, high homogeneity and spongy appearance (Fig. 2a).

Porosity and architecture are relevant factors on the development of scaffolds. These structures must present high surface area and pores with adequate size to lodge the cells. Pore interconnectivity is also important to allow cellular propagation and the diffusion of nutrients and oxygen to the interior of the structure [14,35]. The scaffold micro-structure will also influence the surface properties, swelling, mechanical properties and degradation rate. In Fig. 2b, it is possible to observe the microstructure and pore geometry of the produced scaffolds. The samples present a high porous structure with uniform pore distribution at the surface and in the cross section. While samples treated at 1 V.cm^{-1} and 20 V.cm^{-1} present irregular pore shapes with apparent fracture debris on the surface, the sample treated at 40 V.cm^{-1} show a more regular pore geometry on the surface, a good interconnectivity and thinner walls in the cross sections. The changes on the scaffold's geometry may be the consequence of the different aggregates size and the interactions established during the gelation process, both affected by the EF intensity. This is aligned with previous findings where EF treatments demonstrated the ability to change protein structure and aggregation profiles, originating differentiated network structures with distinctive properties [7,36]. The microstructural changes observed may bring implications on the scaffold's performance regarding cell adhesion and proliferation.

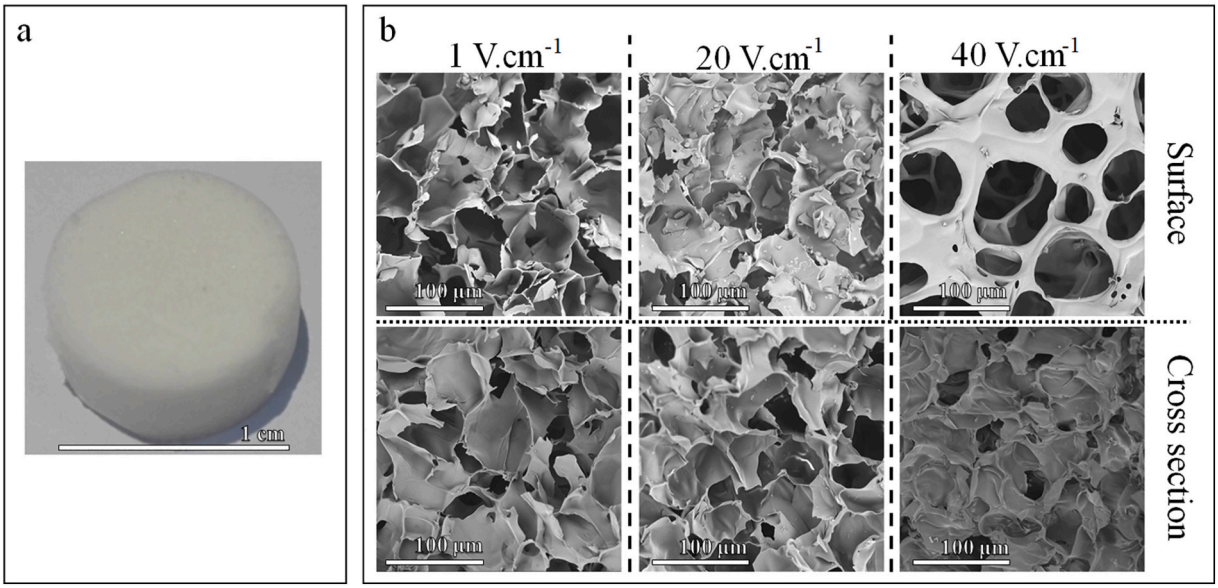

Fig. 2. Representative images of the BSA/casein scaffold produced by OH followed by cold-gelation, a) macroscopic appearance, b) SEM micrographs of the scaffolds surface (top) and cross section (bottom) produced by treatments at 1 V.cm^{-1}, 20 V.cm^{-1} and 40 V.cm^{-1}.

Table 2
Contact angle, swelling ratio and porosity of the obtained scaffolds.

Sample	Contact angle	Swelling ratio	Porosity (%)
1 V.cm^{-1}	92.37 ± 6.80^{a}	8.87 ± 0.22^{a}	84.65 ± 3.38^{a}
20 V.cm^{-1}	95.17 ± 5.94^{a}	9.53 ± 0.18^{b}	88.29 ± 1.35^{ab}
40 V.cm^{-1}	106.39 ± 7.38^{b}	10.03 ± 0.07^{c}	90.89 ± 3.64^{b}

For each column, different letters (a-c) indicate a statistically significant different between samples ($p < 0.05$).

3.2.2. Contact angle, swelling ratio and porosity

The gel forming solutions, temperature, time of treatment and gelation procedure were similar for all tested conditions. Therefore, the differences observed in the scaffolds' properties can only be related with the use of different EF intensities during the OH (i.e. 1, 20 and 40 V.cm^{-1}). In order to further elucidate the effect of EF on scaffolds properties, the contact angle, swelling ratio and porosity of the scaffolds were determined and analysed (Table 2). These properties are related with the contact, uptake and space occupied by the aqueous media in the scaffold's matrix and are therefore critical for scaffolds performance. The contact angle is associated with the surface properties of the scaffolds, therefore influences the scaffold's wettability, the capacity of the scaffold to rehydrate and the cell adhesion [37]. The increase of the EF intensity resulted in an increase of the contact angle, generally caused by the increase of the material's hydrophobicity. It is interesting to note that the sample correspondent to the 40 V.cm^{-1}, with a significantly higher contact angle, also presented a different surface pore geometry. The higher uniformity and apparent integrity on the surface of the scaffold can explain the higher contact angle determined, as the effective surface area in contact with the water drop was higher. It was also determined a positive correlation between EF increase and surface hydrophobicity (ANS binding) of the aggregates' solutions, which implies a higher exposure of hydrophobic groups caused by the EF action. This may affect the type and extent of the network interactions established and surface properties of the scaffolds, helping to explain the differences in morphology and contact angle observed.

After stabilization of the scaffolds in PBS or water, the swelling ratio and porosity were determined. There was a significant ($p < 0.05$) increase on the samples swelling degree with the increase of EF strength. These differences may be the result of the variation in the microstructure or the interactions established with the protein matrix and the aqueous media. The increase of swelling ratio brings a positive implication by facilitating the infiltration of the cells into the scaffolds, increasing the surface area, improving the absorption of fluids, transfer of nutrients and metabolites within the matrix [38]. The porosity reflects the fluid uptake in relation with the volume of the scaffolds. A porous architecture implies a high surface area, contributing to the in and out-flow of nutrients and metabolites, while also allowing higher cell-matrix interactions and cell loading [39]. The variation of the EF causes a change on the scaffolds' porosity, where a positive correlation between the EF and the scaffolds porosity was observed (i.e. higher EF corresponded to higher porosity). The microstructure analysis revealed, especially for sample treated at 40 V.cm^{-1}, a more regular pore distribution with an apparent higher interconnectivity, which would contribute for higher fluid uptake, as well as higher swelling and porosity.

3.2.3. Mechanical properties

After rehydration, the scaffolds were submitted to mechanical tests by compressing them up to 80% of the initial height. This compression did not cause rupture of the scaffolds structure and they returned to the original shape after removing the load. This revealed the high mechanical resistance and flexibility of the obtained structures. Furthermore, the compressive modulus was calculated from the slope of the of the stress-strain curve in the linear region between 10 and 20% strain (Fig. 3). The compression moduli of the scaffolds yielded values between 653 ± 55 and 382 ± 33 Pa, being these values consistent with

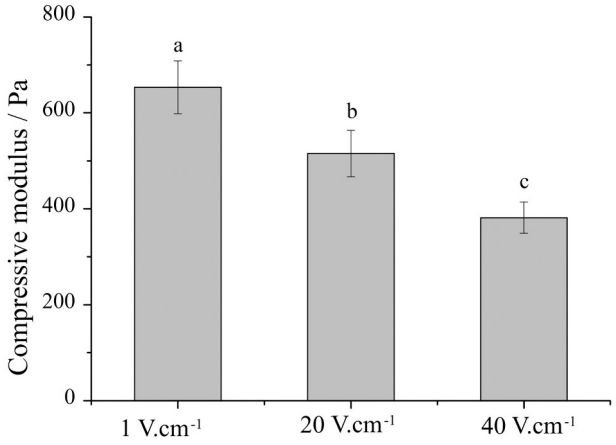

Fig. 3. Compressive modulus of the obtained scaffolds produced trough OH at different EF values. Different letters (a-c) indicate a statistically significant difference between samples ($p < 0.05$).

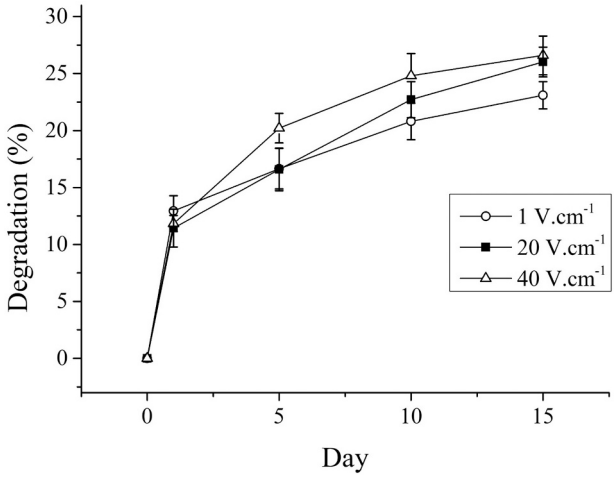

Fig. 4. In vitro degradation rate of the obtained scaffolds, produced by OH treatments at different EF values.

mechanical properties of soft tissues such lung, nervous or connective tissue [40,41]. Moreover, all the samples presented significant differences ($p < 0.05$), being the moduli values inversely correlated with the EF used on the pre-treatments. This reduction can be related with higher swelling and porosity of these samples, as they uptake more fluid and a higher fraction of the samples is composed by aqueous media. The scaffolds' mechanical properties may also contribute to the structural resistance as they are dependent of the characteristic of the "building block" used in the network formation [42]. The previous analysis of the aggregates' suspension used to produce the scaffolds, demonstrated a reduction of the particles size and increase of free SH groups with the EF intensity. The fact that the network was constituted by smaller aggregates can explain the compressive modulus, but given the higher amount of free SH groups, it would be expected to obtain a higher disulphide crosslinking on the scaffolds and thus stronger structures. This was not verified and the swelling and compressive data actually suggest a weaker and more elastic network.

3.2.4. In vitro degradation rate

The degradation rate of a scaffold for tissue engineering is a decisive factor for its application. The material ideally must provide a stable support for cellular proliferation but progressively degrade to allow the tissue to fully form and replace the scaffold [43]. The in vitro

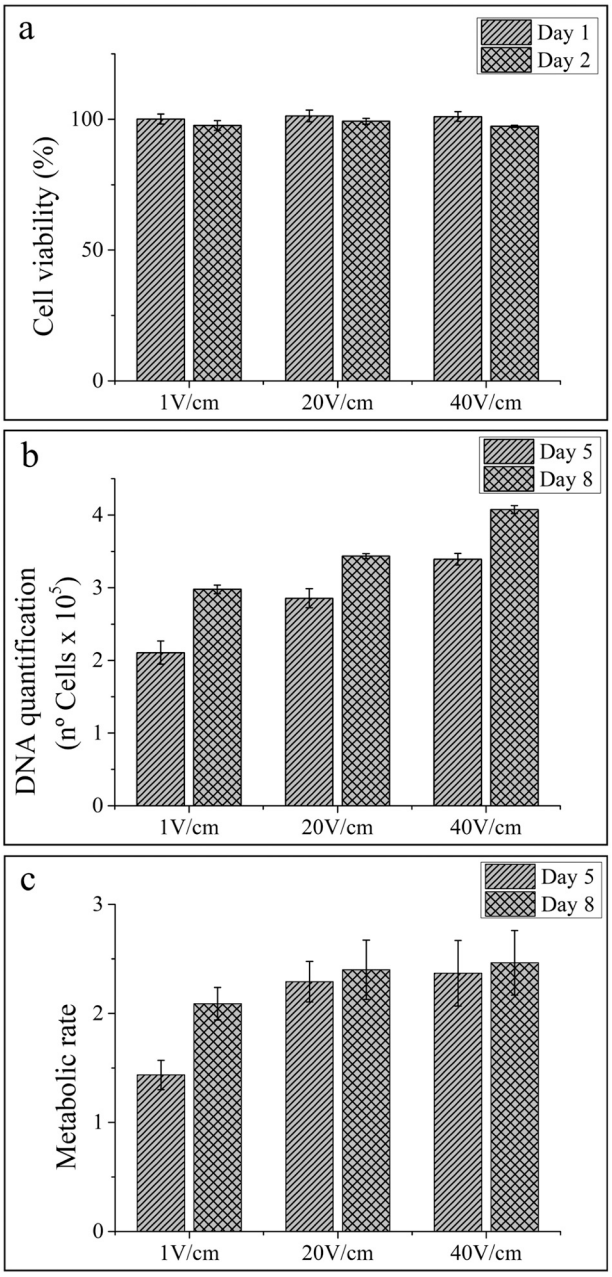

Fig. 5. a) BJ-5ta cell viability measured by MTT assay at 24 and 48 h, b) number of cells on de constructs by DNA quantification, after 5 and 8 days, c) metabolic rate of the cells on the constructs after 5 and 8 days.

degradation of the scaffolds was determined in PBS at 37 °C for a period of 15 days. In Fig. 4, it is possible to observe the degradation profiles along the experimental time, with an initial degradation at day 1 around 12% and above 20% in day 15. The degradation profiles were similar for all the samples, with slight increase in degradation rate with the increase of the EF used during the pre-treatment. The degradation rate was dependent on the physicochemical interaction involved on the network formation and of properties like porosity and swelling degree. The higher porosity and swelling capacity of the samples treated at 20 V.cm^{-1} and 40 V.cm^{-1} may contribute to higher elution of proteins forming the structure and the increase of the degradation rates.

The degradation of the scaffolds is also related with the physicochemical interactions established within the network. The action of the EF in protein aggregation and gelation have demonstrated to change the ratio of disulphide bonds, hydrogen bonds and hydrophobic iterations [36]. Furthermore, during the characterization of the aggregates suspension, it was possible to observe differences in the overall aggregates' properties in response to different EF used during their production. The differences in aggregation and the formation of different physicochemical interactions within the network result on the formation of the structures with different stabilities and degradation rates. Overall, the degradation profile was in line with previous works [22,23] and was adequate to be used as a support for cellular growth.

3.3. Cell viability and proliferation

The biocompatibility of the scaffold's material as well as of its degradation by-products are essential to ensure an adequate performance and should not induce inflammatory response nor cytotoxicity. In order to evaluate the cytotoxicity induced by eluted constituents and by-products from the scaffolds' degradation, BJ-5ta fibroblasts were exposed to a pre-conditioned culture medium by contact with the scaffolds for 24 h. The effect of scaffolds' leachables on cell viability after 24 h and 48 h, evaluated by indirect contact, are presented in Fig. 5a. Regardless of the exposure time, there was no decrease of cellular metabolic activity during the contact with any of the conditioned solutions. These results indicate that none of the scaffolds components presented cytotoxicity for the cells, thus supporting its use for tissue engineering applications. The absence of cellular cytotoxicity using this approach to obtain scaffolds, also represents an improvement facing previous formulation of BSA/casein scaffolds, where cell viability was between 70 and 95%, thus showing a moderate cytotoxicity [22,23]. The improvement in cell viability was probably related with the elimination of DTT from the original formulation. The optimization of the protein processing conditions induced an adequate denaturation and aggregation to form the network, allowing eliminating the use of reducing agents and improving the scaffolds properties. It is also important to highlight that the use of OH and its inherent EF effects do not result in cytotoxicity or negative implications to the cells.

The ability of the scaffolds to support cellular adhesion and proliferation was evaluated by seeding BJ-5ta cells on the scaffolds. The scaffolds/cells were incubated for 5 to 8 days at 37 °C, 5% CO_2 and the cells proliferation was evaluated by DNA quantification (Fig. 5b). It was possible to observe that after 5 days in culture, the samples produced at 1 V.cm^{-1} increased the initial number of cells by 211%. However, for the samples produced at 20 V.cm^{-1} and 40 V.cm^{-1}, the increase of the number of cells on the scaffolds was even higher, presenting proliferation rates of 286% and 334% respectively. After 8 days of culture, the number of cells kept increasing for all the tested scaffolds. Comparing with the initial number of cells, an increase of 298%, 343% and 408% was obtained for scaffolds produced under 1 V.cm^{-1}, 20 V.cm^{-1} and 40 V.cm^{-1}, respectively. Despite the good results observed for the three scaffolds, there was a preferential cell binding/proliferation profile dependent on the scaffold's production conditions. The increasing cell numbers obtained at 1 V.cm^{-1} < 20 V.cm^{-1} < 40 V.cm^{-1} revealed that the scaffolds produced by exposure to higher EF presented higher cell proliferation rates. This can be related with the functionality changes induced by the EF at different intensities, namely the increase of the contact angle, swelling, porosity, degradation rate and elastic behaviour of the scaffolds. The changes in surface properties may facilitate the adhesion of the cells to the matrix, once electrostatic and hydrophobic contributions play a decisive role in such phenomenon [37,44]. Higher swelling and porosity also facilitate the proliferation and dispersion of the cells, as well as allow a better in and out-flow of nutrients, metabolites and gas exchanges [15,38]. The higher degradation rates and lower stiffness of the structure also contribute to the cell proliferation and replacement of the scaffold's matrix with cellular material [35].

The MTS assay is based on the reduction of MTS tetrazolium compound by viable cells to generate a coloured formazan product that is soluble in cell culture media. This conversion is thought to be carried out by NAD(*P*)H-dependent dehydrogenase enzymes in metabolically active

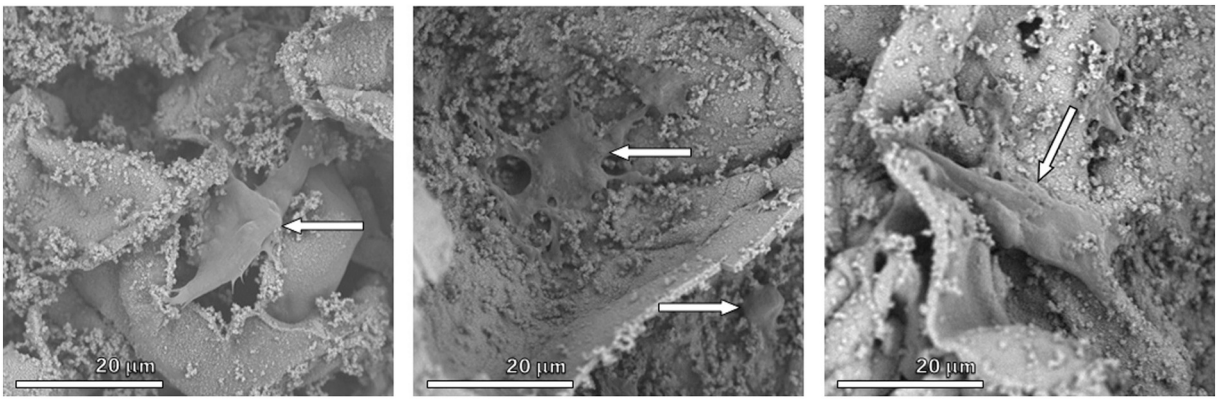

Fig. 6. Representative SEM micrographs of cells adhesion the scaffolds 8 days after seeding, arrows indicate cells positioning.

cells [45] and is not only dependent on the number of viable cells but also on their metabolic activity rate in relation to the standard culture. Considering the direct relation between the DNA quantification and the total number of cells and the MTS assay with metabolic activity of those cells, the relation between these indicators gives back a measure of the relative metabolic rate (Fig. 5c). The results obtained by this analysis demonstrated a higher metabolic activity on the constructs derived from processing at higher EF values. This is particularly relevant if considering that the higher number of cells could imply higher limitation in nutrients and gas exchange, since more volume within the construct was occupied. Nonetheless, the scaffolds' biological performance revealed that a positive correlation could be established between EF effects – leading to higher porosity and swelling, pore architecture and interconnectivity – cellular proliferation and cellular metabolic activity. The specific changes imposed by the EF effects, known to cause structural rearrangement in protein structure and network formation, may also affect the molecular microenvironment within the scaffolds' structure. The changes in surface hydrophobicity of the proteins and of contact angle on the scaffolds' surface are indications of such effects and might as well influence the biochemical activity of the cells. However, this is just a possibility and further studies must be considered to fully elucidate such phenomena.

Cell adhesion and proliferation was confirmed by SEM on dehydrated scaffolds (Fig. 6). In the micrographs, it is possible verify the existence of cells perfectly adhered and included in the scaffold's matrix (white arrows). It was not possible to find differences on the number or adhesion pattern of the cell for the different treatment conditions, nonetheless these possible differentiations might have been dissipated by the drying process prior the observation.

Overall, the results obtained suggested that the BSA/casein scaffolds produced by OH pre-treatment are biocompatible and the application of increasing EF not only results on higher proliferation of cells, but also results in higher metabolic activity of the cells on the constructs.

4. Conclusions

The optimization of the processing conditions during the scaffolds' production allowed to obtain stable structures with adequate functional properties, while avoiding the use of reducing agents. The formation of stable scaffolds' was mostly dependent on the treatment's temperature and duration, while the variation of the EF intensity influenced their functional properties. The obtained scaffolds presented no cytotoxicity to BJ-5ta fibroblast cells and were adequate to support cellular growth. Cell adhesion and proliferation were favoured by the higher surface hydrophobicity, porosity, swelling, elasticity and degradation rates promoted by treatments at higher values of EF. OH demonstrated to be a promising technique to promote protein functionalization and to tune the scaffolds' functional properties, with clear advantages in their biological performance.

CRediT authorship contribution statement

Rui M. Rodrigues: Conceptualization, Investigation, Writing - original draft, Writing - review & editing, Project administration.

Ricardo N. Pereira: Conceptualization, Writing - review & editing Supervision.

António A. Vicente: Conceptualization, Writing - review & editing, Supervision.

Artur Cavaco-Paulo: Writing - review & editing, Supervision.

Artur Ribeiro Conceptualization, Investigation, Writing - original draft, Writing - review & editing, Project administration.

Declaration of competing interest

The authors declare that they have no known competing financial interests or personal relationships that could have appeared to influence the work reported in this paper.

Acknowledgements

This study was supported by the Portuguese Foundation for Science and Technology (FCT) under the scope of the strategic funding of UIDB/04469/2020 unit and BioTecNorte operation (NORTE-01-0145-FEDER000004) funded by the European Regional Development Fund under the scope of Norte2020 - Programa Operacional Regional do Norte.

Appendix A. Supplementary data

Supplementary data to this article can be found online at https://doi.org/10.1016/j.msec.2020.111784.

References

[1] H. De Vries, M. Mikolajczak, J.M. Salmon, J. Abecassis, L. Chaunier, S. Guessasma, D. Lourdin, S. Belhabib, E. Leroy, G. Trystram, Small-scale food process engineering—challenges and perspectives, Innov. Food Sci. Emerg. Technol. 46 (2018) 122–130, https://doi.org/10.1016/j.ifset.2017.09.009.

[2] N. Kaur, A.K. Singh, Ohmic heating: concept and applications—a review, Crit. Rev. Food Sci. Nutr. 56 (2016) 2338–2351, https://doi.org/10.1080/10408398.2013.835303.

[3] C.M.R. Rocha, Z. Genisheva, P. Ferreira-santos, R. Rodrigues, A.A. Vicente, J. A. Teixeira, R.N. Pereira, Bioresource technology electric field-based technologies for valorization of bioresources, Bioresour. Technol. 254 (2018) 325–339, https://doi.org/10.1016/j.biortech.2018.01.068.

[4] S. Sastry, Ohmic heating and moderate electric field processing, Food Sci. Technol. Int. 14 (2008) 419–422, https://doi.org/10.1177/1082013208098813.

[5] M.C. Knirsch, C. dos Santos, A.A. de Oliveira Soares Vicent, T.C. Vessoni Penna, C. Alves dos Santos, A.A. Martins de Oliveira Soares Vicent, T.C. Vessoni Penna, A.A. Martins de Oliveira Soares Vicente, T.C. Vessoni Penna, C. dos Santos, A.A. de

Oliveira Soares Vicente, T.C. Vessoni Penna, Ohmic heating – a review, Trends Food Sci. Technol. 21 (2010) 436–441. doi:https://doi.org/10.1016/j.tifs.2010.06.003.
[6] R.M. Rodrigues, L.H. Fasolin, Z. Avelar, S.B. Petersen, A.A. Vicente, R.N. Pereira, Y. Zheng, Z. Li, C. Zhang, B. Zheng, Y. Tian, Effects of moderate electric fields on cold-set gelation of whey proteins – from molecular interactions to functional properties, Food Hydrocoll. 101 (2020). doi:https://doi.org/10.1016/j.foodhyd.2019.105505.
[7] R.N. Pereira, R.M. Rodrigues, O.L. Ramos, F.X. Malcata, J.A. Teixeira, A.A. Vicente, Production of whey protein-based aggregates under ohmic heating, Food Bioprocess Technol. 9 (2016) 576–587, https://doi.org/10.1007/s11947-015-1651-4.
[8] R.M. Rodrigues, A.J. Martins, O.L. Ramos, F.X. Malcata, J.A. Teixeira, A.A. Vicente, R.N. Pereira, Influence of moderate electric fields on gelation of whey protein isolate, Food Hydrocoll. 43 (2015) 329–339, https://doi.org/10.1016/j.foodhyd.2014.06.002.
[9] R.M. Rodrigues, A.A. Vicente, S.B. Petersen, R.N. Pereira, Electric field effects on β-lactoglobulin thermal unfolding as a function of pH – impact on protein functionality, Innov. Food Sci. Emerg. Technol. 52 (2019) 1–7, https://doi.org/10.1016/j.ifset.2018.11.010.
[10] N. Celikkin, C. Rinoldi, M. Costantini, M. Trombetta, A. Rainer, W. Święszkowski, Naturally derived proteins and glycosaminoglycan scaffolds for tissue engineering applications, Mater. Sci. Eng. C. 78 (2017) 1277–1299, https://doi.org/10.1016/j.msec.2017.04.016.
[11] M. Gebauer, A. Skerra, Engineered protein scaffolds as next-generation therapeutics, Annu. Rev. Pharmacol. Toxicol. 60 (2020) 391–415, https://doi.org/10.1146/annurev-pharmtox-010818-021118.
[12] A.C. Schloss, D.M. Williams, L.J. Regan, Protein-Based Hydrogels for Tissue Engineering, in: 2016: pp. 167–177. doi:https://doi.org/10.1007/978-3-319-39196-0_8.
[13] S. Khanna, A.K. Singh, S.P. Behera, S. Gupta, Thermoresponsive BSA hydrogels with phase tunability, Mater. Sci. Eng. C. 119 (2021) 111590, https://doi.org/10.1016/j.msec.2020.111590.
[14] T. Weigel, G. Schinkel, A. Lendlein, Design and preparation of polymeric scaffolds for tissue engineering, Expert Rev. Med. Devices. 3 (2006) 835–851, https://doi.org/10.1586/17434440.3.6.835.
[15] A. Eltom, G. Zhong, A. Muhammad, Scaffold techniques and designs in tissue engineering functions and purposes: a review, Adv. Mater. Sci. Eng. 2019 (2019), https://doi.org/10.1155/2019/3429527.
[16] J.L. Drury, D.J. Mooney, Hydrogels for tissue engineering: scaffold design variables and applications, Biomaterials. 24 (2003) 4337–4351, https://doi.org/10.1016/S0142-9612(03)00340-5.
[17] V. Charulatha, A. Rajaram, Influence of different crosslinking treatments on the physical properties of collagen membranes, Biomaterials. 24 (2003) 759–767, https://doi.org/10.1016/S0142-9612(02)00412-X.
[18] S. Amin, G.V. Barnett, J.A. Pathak, C.J. Roberts, P.S. Sarangapani, Protein aggregation, particle formation, characterization & rheology, Curr. Opin. Colloid Interface Sci. 19 (2014) 438–449, https://doi.org/10.1016/j.cocis.2014.10.002.
[19] E.Y. Chi, S. Krishnan, T.W. Randolph, J.F. Carpenter, Physical stability of proteins in aqueous solution: mechanism and driving forces in nonnative protein aggregation, Pharm. Res. 20 (2003) 1325–1336, https://doi.org/10.1023/A:1025771421906.
[20] K. Ako, T. Nicolai, D. Durand, Salt-induced gelation of globular protein aggregates: structure and kinetics, Biomacromolecules. 11 (2010) 864–871, https://doi.org/10.1021/bm9011437.
[21] C.M. Bryant, D.J. McClements, Molecular basis of protein functionality with special consideration of cold-set gels derived from heat-denatured whey, Trends Food Sci. Technol. 9 (1998) 143–151, https://doi.org/10.1016/S0924-2244(98)00031-4.
[22] A. Ribeiro, A.C. Gomes, A.M. Cavaco-Paulo, Developing scaffolds for tissue engineering using the Ca2+-induced cold gelation by an experimental design approach, J. Biomed. Mater. Res. Part B Appl. Biomater. 100B (2012) 2269–2278, https://doi.org/10.1002/jbm.b.32797.
[23] A. Ribeiro, V. Volkov, M.B. Oliveira, J. Padrão, J.F. Mano, A.C. Gomes, A. Cavaco-Paulo, BSA/HSA ratio modulates the properties of Ca2+-induced cold gelation scaffolds, Int. J. Biol. Macromol. 89 (2016) 535–544, https://doi.org/10.1016/j.ijbiomac.2016.05.012.
[24] H. Yan, A. Saiani, J.E. Gough, A.F. Miller, Thermoreversible protein hydrogel as cell scaffold, Biomacromolecules. 7 (2006) 2776–2782, https://doi.org/10.1021/bm0605560.
[25] B. Li, K. Ren, Y. Wang, Y. Qi, X. Chen, Y. Huang, Protein-cross-linked hydrogels with tailored swelling and bioactivity performance: a comparative study, ACS Appl. Mater. Interfaces 8 (2016) 30788–30796, https://doi.org/10.1021/acsami.6b11287.
[26] M.E. Solovieva, V.V. Solovyev, A.A. Kudryavtsev, Y.A. Trizna, V.S. Akatov, Vitamin B12b enhances the cytotoxicity of dithiothreitol, Free Radic. Biol. Med. 44 (2008) 1846–1856, https://doi.org/10.1016/j.freeradbiomed.2008.02.002.
[27] P.A. Thibodeau, S. Kocsis-Bédard, J. Courteau, T. Niyonsenga, B. Paquette, Thiols can either enhance or suppress DNA damage induction by catecholestrogens, Free Radic. Biol. Med. 30 (2001) 62–73, https://doi.org/10.1016/S0891-5849(00)00446-9.
[28] I.E.K. and K.D.H. L. Tartier, Y.L. McCarey, J.E. Biaglow, Apoptosis induced by dithiothreitol in HL-60 cells shows early activation of caspase 3 and is independent of mitochondria, in: Cell Death Differ, 2000: pp. 1002–1010.
[29] R.M. Rodrigues, A.A. Vicente, S.B. Petersen, R.N. Pereira, Electric field effects on β-lactoglobulin thermal unfolding as a function of pH – impact on protein functionality, Innov. Food Sci. Emerg. Technol. 52 (2019) 1–7, https://doi.org/10.1016/j.ifset.2018.11.010.
[30] L. Vera Candioti, M.M. De Zan, M.S. Cámara, H.C. Goicoechea, Experimental design and multiple response optimization. Using the desirability function in analytical methods development, Talanta. 124 (2014) 123–138. doi:https://doi.org/10.1016/j.talanta.2014.01.034.
[31] G.L. Ellman, K.D. Courtney, V. Andres, R.M. Featherstone, A new and rapid colorimetric determination of acetylcholinesterase activity, Biochem. Pharmacol. 7 (1961) 88–95, https://doi.org/10.1016/0006-2952(61)90145-9.
[32] Y. Liu, D. Schubert, Cytotoxic amyloid peptides inhibit cellular 3-(4,5-dimethylthiazol-2-yl)-2,5-diphenyltetrazolium bromide (MTT) reduction by enhancing MTT formazan exocytosis, J. Neurochem. 69 (2002) 2285–2293, https://doi.org/10.1046/j.1471-4159.1997.69062285.x.
[33] Ö.S. Aslantürk, In vitro cytotoxicity and cell viability assays: principles, advantages, and disadvantages, in: Genotoxicity - A Predict. Risk to Our Actual World, InTech, 2018, https://doi.org/10.5772/intechopen.71923.
[34] D.Y. Mang, A.B. Abdou, N.Y. Njintang, E.J.M. Djiogue, B.B. Loura, M.C. Mbofung, Application of desirability-function and RSM to optimize antioxidant properties of mucuna milk, J. Food Meas. Charact. 9 (2015) 495–507, https://doi.org/10.1007/s11694-015-9258-z.
[35] F.J. O'Brien, Biomaterials & scaffolds for tissue engineering, Mater. Today 14 (2011) 88–95, https://doi.org/10.1016/S1369-7021(11)70058-X.
[36] R.M. Rodrigues, L.H. Fasolin, Z. Avelar, S.B. Petersen, A.A. Vicente, R.N. Pereira, Effects of moderate electric fields on cold-set gelation of whey proteins – from molecular interactions to functional properties, Food Hydrocoll. 101 (2020). doi: https://doi.org/10.1016/j.foodhyd.2019.105505.
[37] S.H. Kim, H.J. Ha, Y.K. Ko, S.J. Yoon, J.M. Rhee, M.S. Kim, H.B. Lee, G. Khang, Correlation of proliferation, morphology and biological responses of fibroblasts on LDPE with different surface wettability, J. Biomater. Sci. Polym. Ed. 18 (2007) 609–622, https://doi.org/10.1163/156856207780852514.
[38] M. Peter, N.S. Binulal, S.V. Nair, N. Selvamurugan, H. Tamura, R. Jayakumar, Novel biodegradable chitosan–gelatin/nano-bioactive glass ceramic composite scaffolds for alveolar bone tissue engineering, Chem. Eng. J. 158 (2010) 353–361, https://doi.org/10.1016/j.cej.2010.02.003.
[39] G. Chen, N. Kawazoe, Preparation of polymer scaffolds by ice particulate method for tissue engineering, in: Biomater. Nanoarchitectonics, Elsevier, 2016, pp. 77–95, https://doi.org/10.1016/B978-0-323-37127-8.00006-6.
[40] C.F. Guimarães, L. Gasperini, A.P. Marques, R.L. Reis, The stiffness of living tissues and its implications for tissue engineering, Nat. Rev. Mater. 5 (2020) 351–370, https://doi.org/10.1038/s41578-019-0169-1.
[41] F. Rehfeldt, A. Engler, A. Eckhardt, F. Ahmed, D. Discher, Cell responses to the mechanochemical microenvironment—implications for regenerative medicine and drug delivery☆, Adv. Drug Deliv. Rev. 59 (2007) 1329–1339, https://doi.org/10.1016/j.addr.2007.08.007.
[42] A.C. Alting, R.J. Hamer, C.G. De Kruif, R.W. Visschers, Cold-set globular protein gels: interactions, structure and rheology as a function of protein concentration, J. Agric. Food Chem. 51 (2003) 3150–3156, https://doi.org/10.1021/jf0209342.
[43] S. Gomes, I.B. Leonor, J.F. Mano, R.L. Reis, D.L. Kaplan, Natural and genetically engineered proteins for tissue engineering, Prog. Polym. Sci. 37 (2012) 1–17, https://doi.org/10.1016/j.progpolymsci.2011.07.003.
[44] M. Burke, J.P.K. Armstrong, A. Goodwin, R.C. Deller, B.M. Carter, R.L. Harniman, A. Ginwalla, V.P. Ting, S.A. Davis, A.W. Perriman, Regulation of scaffold cell adhesion using artificial membrane binding proteins, Macromol. Biosci. 17 (2017) 1600523, https://doi.org/10.1002/mabi.201600523.
[45] G. Malich, B. Markovic, C. Winder, The sensitivity and specificity of the MTS tetrazolium assay for detecting the in vitro cytotoxicity of 20 chemicals using human cell lines, Toxicology. 124 (1997) 179–192, https://doi.org/10.1016/S0300-483X(97)00151-0.